

Characteristics of Complexes Composed of Sodium Hyaluronate and Bovine Serum Albumin

Shouhong XU, Junpei YAMANAKA, Shizuko SATO, Isamu MIYAMA, and Masakatsu YONESE*

Faculty of Pharmaceutical Sciences, Nagoya City University, 3-1 Tanabe-dori, Mizuho-ku, Nagoya 467-8603, Japan.

Received September 10, 1999; accepted February 11, 2000

Complexes composed of sodium hyaluronate (NaHA) and bovine serum albumin (BSA) were studied to elucidate the exact composition of the complex, the phase separation, the electrophoretic mobility and the size using dynamic light scattering (DLS) and electrophoretic light scattering (ELS), *etc.* The phase diagram of the mixed solutions was determined. The complexes were soluble in neutral or weakly acidic pH regions and showed phase separation in the more acidic pH region. From the concentration of Na^+ released from NaHA when it binds to BSA, the ratios of BSA to NaHA of the complexes were determined. In the region of soluble complexes, one BSA molecule was determined to bind with 15 carboxylic groups of NaHA and in the region of insoluble complexes to bind with 6 carboxylic groups. At the phase separation point, 117 BSA molecules bound with one NaHA molecule and 17% of the carboxylic groups of NaHA did not contribute to the binding of BSA. The sizes of the complexes decreased from several μm to several hundred nm as the binding ratio of BSA increases. Decreases in the viscosities of the mixed solutions were consistent with the decreases of the sizes. From these results, a model of complex formation is proposed.

Key words sodium hyaluronate; bovine serum albumin; complex; light scattering

Complexes of polyelectrolytes and proteins have been studied to understand the structures and the mechanism of their formation from basic and applied points of view.^{1–12)} Complex formation due to electrostatic interactions between oppositely charged groups depends on pH, ion strength, concentration and temperature. According to Kokufuta E. *et al.*,³⁾ the complexes are grouped into intra- and inter-polymer complexes. The former is a soluble complex and the latter is formed by the bindings of the intra-polymer complexes. The inter-polymer complexes bring about a phase separation, and precipitated aggregations or coacervations are formed. Polyanions and proteins form soluble complexes in neutral or weak acidic pH region, and in the more acidic pH region, a phase separation occurs.

Complexes composed of a mucopolysaccharide and a protein have been widely studied to elucidate the functions in the living and as basic studies of the interaction between polyelectrolytes. Hyaluronate (HA) is widely distributed in living tissue, such as skin, bone, glass body fluid, *etc.* It does not exist alone and usually combines with protein to maintain the shape of the tissues and to control the permeability of ions and water. The structure of HA is a linear polysaccharide whose repeating disaccharide units are composed of *N*-acetyl-D-glucosamine and D-glucuronic acid, and there is only one carboxylic group per one repeating unit.^{13,14)} HA is well known to moisturize skin to prevent aging and is used widely in the cosmetics and pharmaceutical industry.¹⁵⁾

In our laboratory, the characteristics of polysaccharides have been studied not only in solutions but also at interfaces to elucidate the effects of charge densities and the kinds of charged groups. Recently, NaHA was reported to form two-dimensional auto-organized hexagonal-like networks on a bovine serum albumin (BSA) monolayer resulting from interfacial interactions.¹⁶⁾ In this paper, the interactions of sodium hyaluronate (NaHA) and BSA in solution were studied as the basis of interfacial interactions. Their complex formation, the composition, the size and the phase separation were studied using dynamic light scattering (DLS) and elec-

trophoretic light scattering (ELS) which are powerful techniques in the study of macromolecular solutions.^{17,18)}

Experimental

Materials and Sample Preparation NaHA obtained from Seikagaku Kogyo Co. Ltd. was used without any purification. The weight averaged molecular weight M_w was determined to be $8.50 \times 10^5 \text{ g} \cdot \text{mol}^{-1}$ using static light scattering (Otsuka Electronics Co., DLS-700Ar).

BSA was purified by delipidizing a BSA Fraction V (Seikagaku Kogyo) as follows: 1) To the BSA solution (10 w/v%, 100 cm^3), an activated carbon (5 g, Darco Ci.Ltd., G-60) was added. 2) After adjusting the solution to pH=3, the solution was stirred in an ice bath for 2 h, and then centrifuged under $24000 \times g$ for 30 min. 3) The supernatant was filtered and adjusted to pH=5 by adding NaOH ($0.2 \text{ mol} \cdot \text{dm}^{-3}$). 4) The above solution was passed through a mixed column (cation exchange resin: anion exchange resin=1:1) and then freeze-dried. Cation and anion exchange resins were of Amberlite IR-120B and IRA-400 (Organo Co.). The isoionic point of BSA was 5.2 and the value of M_w was $70000 \text{ g} \cdot \text{mol}^{-1}$.

Preparing sample solutions composed of NaHA and BSA, concentration of NaHA (C_{NaHA}) was 0.1 w/v% ($1.2 \mu\text{mol} \cdot \text{dm}^{-3}$) and various concentrations of BSA were added.

Measurement of Activities of Na^+ and pH of Mixed Solutions Composed of NaHA and BSA The activities of Na^+ ion of NaHA solution and of NaHA–BSA mixed solutions were measured at 25 °C using a pH/ion meter (Orion 920A), which was connected with a double junction reference electrode (Orion Co., No. 900200). The pH value was obtained by using a digital pH/mV meter (Orion model 701A). The ionic strengths I of the solutions were $0.001 \text{ mol} \cdot \text{dm}^{-3}$, which was adjusted by NaCl.

Measurement of Viscosity and Transparency The viscosities of NaHA–BSA mixed solutions were measured at 25 °C under the condition of $J=0.001 \text{ mol} \cdot \text{dm}^{-3}$ using an Ostward-type viscometer of which the falling time of the solvent was 92 s. The transparencies of the solutions were measured in the region from neutral to acidic pH region using a spectrophotometer (Hitachi Electronics Co., U-3000) at $\lambda=700 \text{ nm}$.

Measurement of Electrophoretic Mobility, Apparent Diffusion Coefficient and Hydrodynamic Diameter The electrophoretic mobilities of NaHA–BSA mixed solutions were measured at 25 °C using an electrophoretic light scattering photometer (Otsuka Electronics Co., LEZA-600, $\lambda=632.8 \text{ nm}$) at a fixed scattering angle of 20°. The true mobility U was obtained by correcting for the electro-osmotic effects. The apparent diffusion coefficients of the NaHA–BSA mixed solutions were measured at 25 °C in the region of scattering angle $\lambda=30\text{--}90^\circ$ using a DLS (DLS700Ar: Otsuka Electronics Co., $\lambda=488 \text{ nm}$).

* To whom correspondence should be addressed. e-mail: yonese@phar.nagoya-cu.ac.jp

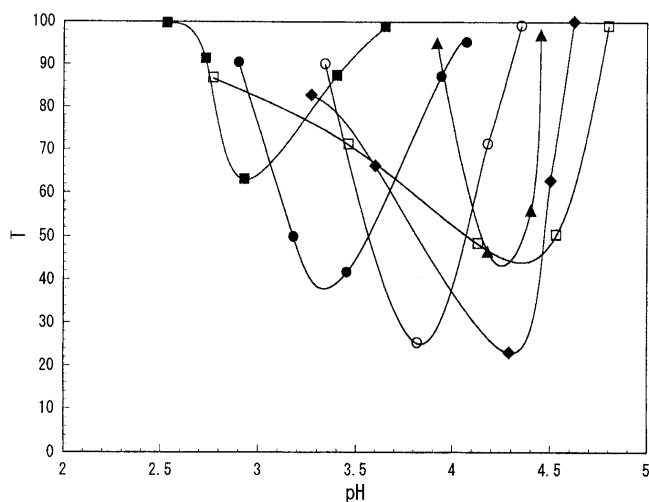


Fig. 1. Transparencies of NaHA-BSA Mixed Solutions Plotted against pH Value

$C_{\text{NaHA}} = 1.2 \mu\text{mol} \cdot \text{dm}^{-3}$, $J = 0.001 \text{ mol} \cdot \text{dm}^{-3}$. $C_{\text{BSA}} (\mu\text{mol} \cdot \text{dm}^{-3})$: ■, 15; ●, 29; ○, 42; ▲, 57; ◆, 85; □, 128.

Results

Soluble and Insoluble Complexes Various amounts of BSA ($C_{\text{BSA}} = 0-128 \mu\text{mol} \cdot \text{dm}^{-3}$) were added to NaHA solution ($C_{\text{NaHA}} = 1.2 \mu\text{mol} \cdot \text{dm}^{-3}$, $J = 0.001 \text{ mol} \cdot \text{dm}^{-3}$) and then the mixed solutions were titrated by using HCl ($1 \text{ mol} \cdot \text{dm}^{-3}$).²⁾ The transparency (T) of the solutions was measured under stirring at 25°C . As shown in Fig. 1, with decreasing pH the solutions became turbid due to the formation of the insoluble complexes and the T of the mixed solutions showed minima at which the complexes started to precipitate. In the more acidic pH region, the precipitation increased and became more bulky. As a result, the solutions became less turbid. The pH value at which T began to decrease was defined as the phase separation pH (pH_{ps}), and the pH value at which T showed a minimum was defined as the precipitation pH (pH_{pr}). The values of pH_{ps} and pH_{pr} depended significantly on C_{BSA} and increased with increasing C_{BSA} .³⁾

Complex formations and the states depended on pH and the compositions. The values of pH_{ps} and pH_{pr} are shown in Fig. 2 as a function of C_{BSA} . In the region of III, the precipitation of the complex occurs and in the region of II the insoluble complexes are dispersed. In the region of I, the soluble complexes are considered to be formed. In the more alkaline region, the complexes cannot be formed although the boundary was not determined.

Concentration of Na^+ Ion Released Due to Complex Formation In the formation of the complexes between NaHA and BSA, the complexes are considered to be formed by an electrostatic interaction between carboxylic groups of NaHA and BSA. When BSA binds to NaHA, Na^+ ions should be released. The activities of Na^+ ion of the mixed solutions composed of NaHA ($C_{\text{NaHA}} = 1.2 \mu\text{mol} \cdot \text{dm}^{-3}$) and BSA ($C_{\text{BSA}} = 0-171 \mu\text{mol} \cdot \text{dm}^{-3}$) were measured under $J = 0.001 \text{ mol} \cdot \text{dm}^{-3}$ by using a Na^+ ion electrode at 25°C . The activity coefficients were approximated to be 1 because of the low concentration.

Figure 3 shows the concentration of Na^+ ion of the mixed solutions (C_{Na^+}), released by the binding of BSA to NaHA as a function of C_{BSA} . The value of C_{Na^+} at $C_{\text{BSA}} = 0$ is the contribution of NaHA and NaCl. With increasing C_{BSA} , C_{Na^+} in-

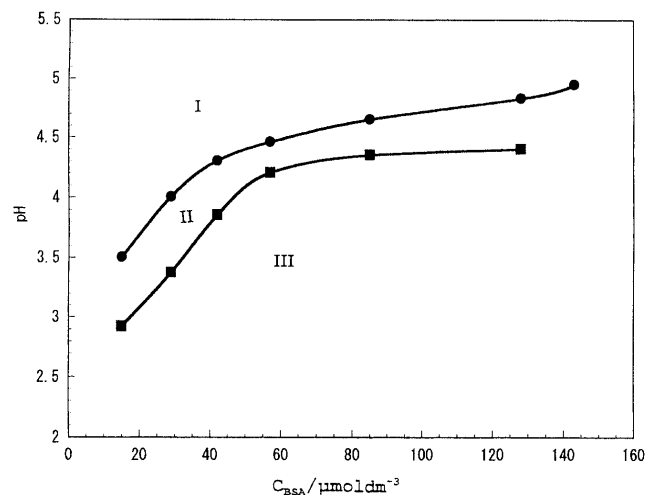


Fig. 2. Phase Diagram of Soluble and Insoluble Complexes

■, pH_{pr} , pH which the insoluble complex begins to precipitate; ●, pH_{ps} , pH which the phase separation begins to occur. I, soluble complex; II, suspended complex; III, precipitating complex.

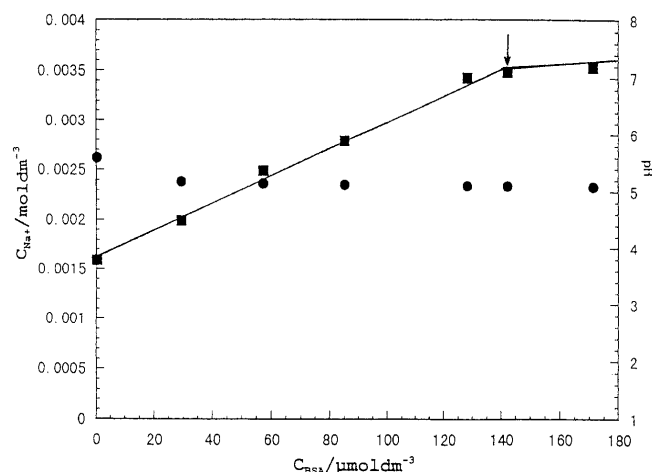


Fig. 3. Concentration of Na^+ Ion Released from NaHA by Adding BSA

■, concentration of Na^+ ion; ●, the pH value of mixed solution. $C_{\text{NaHA}} = 1.2 \mu\text{mol} \cdot \text{dm}^{-3}$, $J = 0.001 \text{ mol} \cdot \text{dm}^{-3}$ (NaCl). The arrow shows C_{BSA} at which the solution became turbid.

creased due to the increases in the binding amounts of BSA. In the region of $C_{\text{BSA}} \geq 141 \mu\text{mol} \cdot \text{dm}^{-3}$, the solutions became a little turbid due to the formation of the insoluble complex. An arrow in Fig. 3 shows the phase separation point. The slopes of C_{Na^+} changed at $C_{\text{BSA}} = 141 \mu\text{mol} \cdot \text{dm}^{-3}$ and in the region of $C_{\text{BSA}} \geq 141 \mu\text{mol} \cdot \text{dm}^{-3}$ the slope decreased significantly. These results show the binding states of BSA change at the phase separation point, i.e., the numbers of carboxylic group of NaHA binding to one BSA molecule changed. At $C_{\text{BSA}} = 141 \mu\text{mol} \cdot \text{dm}^{-3}$, the ratio of C_{BSA} to C_{NaHA} ($C_{\text{BSA}}/C_{\text{NaHA}}$)^{ps} was 117.

The values of pH of the mixed solutions are also shown in Fig. 3. As C_{BSA} increased, pH of the solutions decreased slightly from the value of pH of NaHA solution ($\text{pH} = 5.6$) to $\text{pH} = 5.0$.

Viscosity of Mixed Solutions Effects of the complex formation on the viscosity of the mixed solutions were studied by using an Ostward-type viscometer under the same conditions mentioned above. The relative viscosities of the soluble solutions (η_{rel}) were measured and the results are

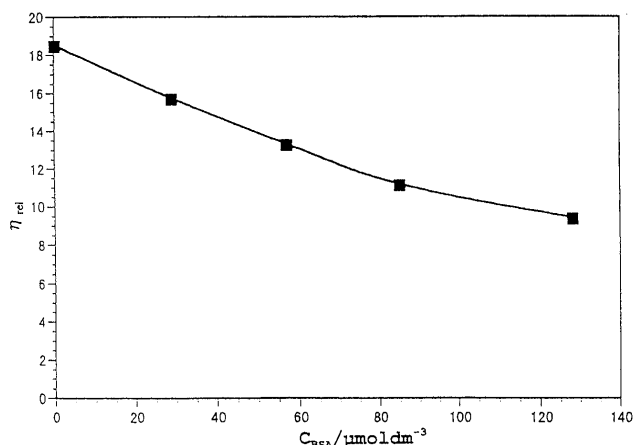


Fig. 4. Relative Viscosity of Soluble Complexes Plotted against C_{BSA}
 $C_{\text{NaHA}} = 1.2 \mu\text{mol} \cdot \text{dm}^{-3}$, $J = 0.001 \text{ mol} \cdot \text{dm}^{-3}$.

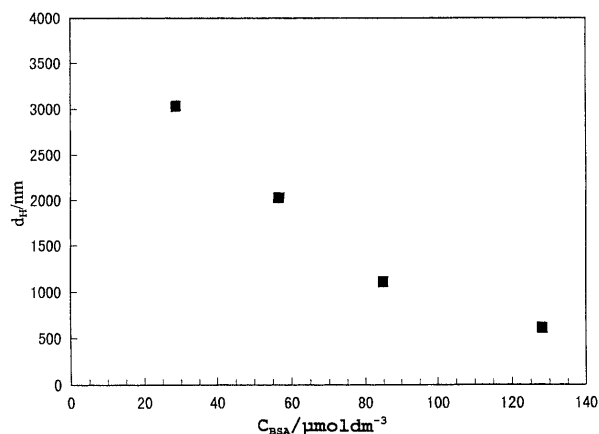


Fig. 6. Hydrodynamic Diameter of Complex Particles Plotted against C_{BSA}

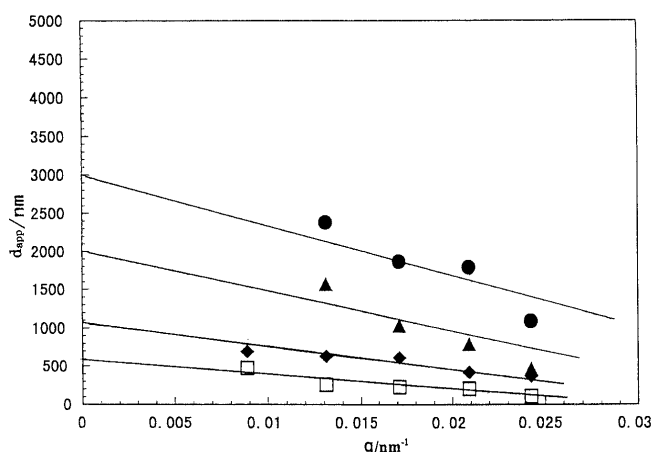


Fig. 5. Apparent Diameter of Complex Particles Plotted against Scattering Vector q

$C_{\text{NaHA}} = 1.2 \mu\text{mol} \cdot \text{dm}^{-3}$, $J = 0.001 \text{ mol} \cdot \text{dm}^{-3}$. $C_{\text{BSA}} (\mu\text{mol} \cdot \text{dm}^{-3})$: ●, 29; ▲, 57; ◆, 85; □, 128.

shown in Fig. 4 as a function of C_{BSA} . In the region of $C_{\text{BSA}} \geq 141 \mu\text{mol} \cdot \text{dm}^{-3}$, the viscosities were not measured because of the phase separation of the solutions. The values of η_{rel} were found to decrease with increasing C_{BSA} , *i.e.*, in spite of the increases of the binding amounts of BSA to NaHA the values of η_{rel} were found to decrease. NaHA molecules are known to have a worm like structure¹⁹ in solution due to electrostatic repulsion. Thus, with increasing C_{BSA} , NaHA-BSA complexes are considered to change from the extended worm like structure to a shrunken random coil structure.

Apparent Diffusion Coefficient and Diameter of Complexes To estimate the sizes of the NaHA-BSA complexes, their apparent diffusion coefficients (D_{app}) were measured using DLS in the region of scattering angle $\theta = 30^\circ$ – 90° . The values of D_{app} were obtained by the cumulant method. The variances were in the range of 0.3–0.7 which were much more than 0.02 and the size distributions of the complexes were found to be inhomogeneous. Assuming that all the complexes are sphere-like structures, their mean apparent diameters (d_{app}) were estimated by using the Einstein-Stokes' equation. The results of d_{app} are shown in Fig. 5 as a function of scattering vector (q) ($q = 4\pi n/\lambda \sin(\theta/2)$), where λ is wavelength. The values of d_{app} depended on q and decreased

with increasing q . The dependence results from long range interactions between the complexes and the hydrodynamic diameter d_{H} can be obtained from the extrapolated value of d_{app} to $q=0$.²⁰ As shown in Fig. 6, the values of d_{H} decreased from 3 μm to 600 nm with increasing C_{BSA} . The decrease of d_{H} with increasing C_{BSA} was consistent with the results of decreasing η_{rel} shown in Fig. 4. As to the point at $C_{\text{BSA}}=0$, the value of D_{app} could not be measured. The size of the NaHA molecule is considered to be too large to be measured.

Electrophoretic Mobility of Complexes The electrophoretic mobilities (U) of the complexes in the same mixed solutions mentioned above were measured using ELS at 25 $^\circ\text{C}$. The spectra U of $C_{\text{BSA}} = 57 \mu\text{mol} \cdot \text{dm}^{-3}$ is shown in Fig. 7(a) as a typical result in the region of $C_{\text{BSA}} < C_{\text{BSA}}^{\text{ps}}$. The spectra showed one sharp peak. As shown in a previous paper,²¹ the isoelectric point of BSA was $\text{pH} = 5.2$ and the values of U of BSA were almost 0 in the region of $\text{pH} = 5.6$ – 5.0 . The peak of BSA was not found near 0. The spectrum of $C_{\text{BSA}} = 128 \mu\text{mol} \cdot \text{dm}^{-3}$, which is a little less than $C_{\text{BSA}}^{\text{ps}}$, is shown in Fig. 7 (b) and showed a slightly broad peak with several small shoulders at the region near $U=0$. The shoulders show the presence of the complexes containing more BSA being just before the phase separation. However, the peak of BSA could be neglected. From these results, almost all BSA molecules added to NaHA solutions are considered to bind to NaHA molecules in the region of $C_{\text{BSA}} < C_{\text{BSA}}^{\text{ps}}$.^{4,5}

The results U of the complexes are shown in Fig. 8 as a function of C_{BSA} . The results of U were negative and the absolute values of U decreased with increasing C_{BSA} in the region of $C_{\text{BSA}} < C_{\text{BSA}}^{\text{ps}}$. The value of $C_{\text{BSA}}=0$ is that of NaHA ($U = -4.982 \times 10^4 \text{ cm}^2 \cdot \text{V}^{-1} \cdot \text{s}^{-1}$). In the region of $C_{\text{BSA}} \geq C_{\text{BSA}}^{\text{ps}}$, in which the phase separation occurred, the mobilities were measured after filtrating out insoluble complexes through a $0.8 \mu\text{m}$ filter. However, several peaks appeared near the main peaks in the filtrates. The values of U of the main peak are shown in Fig. 8 as an open square and the results increased slightly. Even after filtering, inhomogeneous complexes were found to exist and the values of U of the main complexes are considered to increase due to the slight increases of binding BSA in $C_{\text{BSA}} \geq C_{\text{BSA}}^{\text{ps}}$ as shown in Fig. 3. It should be noted that the value of U of $C_{\text{BSA}}^{\text{ps}}$ was negative $-1.9 \times 10^4 \text{ cm}^2 \cdot \text{V}^{-1} \cdot \text{s}^{-1}$.

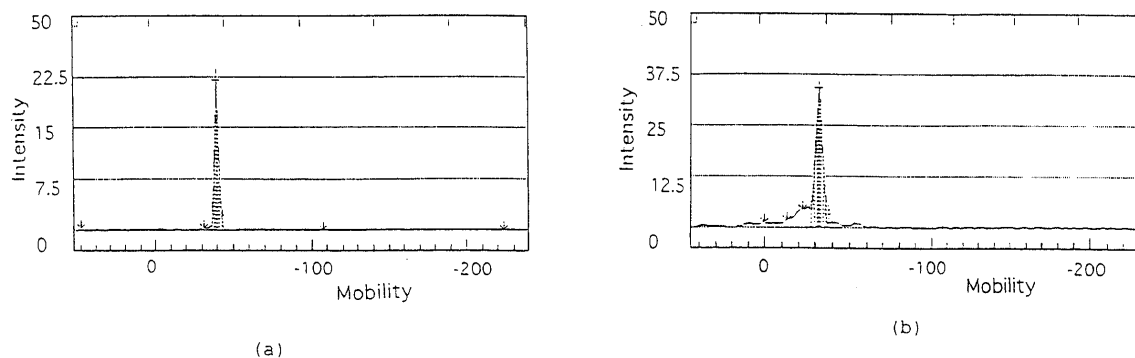


Fig. 7. Spectra of Mobility of Soluble NaHA-BSA Complexes

(a) $C_{\text{NaHA}} = 1.2 \mu\text{mol} \cdot \text{dm}^{-3}$, $C_{\text{BSA}} = 57 \mu\text{mol} \cdot \text{dm}^{-3}$, $n_{\text{BSA}}/n_{\text{NaHA}} = 47$. (b) $C_{\text{NaHA}} = 1.2 \mu\text{mol} \cdot \text{dm}^{-3}$, $C_{\text{BSA}} = 128 \mu\text{mol} \cdot \text{dm}^{-3}$, $n_{\text{BSA}}/n_{\text{NaHA}} = 107$.

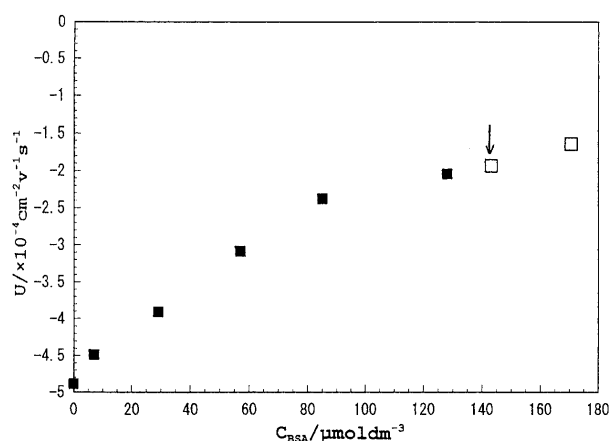


Fig. 8. Electrophoretic Mobility of Soluble Complexes Plotted against C_{BSA}

$C_{\text{NaHA}} = 1.2 \mu\text{mol} \cdot \text{dm}^{-3}$, $J = 0.001 \text{mol} \cdot \text{dm}^{-3}$ (NaCl). The arrow shows C_{BSA} at which the solution became turbid.

Discussion

The Composition of Soluble Complexes The formation of the complex between NaHA and BSA brings about the release of Na^+ ions according to the following reaction.⁶⁾



Where n is the molar numbers of the carboxylic groups of NaHA bound to one mole BSA. Assuming all BSA molecules added to NaHA solution bind to NaHA molecules in the region of $C_{\text{BSA}} \leq C_{\text{BSA}}^{\text{ps}}$, n can be obtained from Eq. 2,

$$n = \Delta C_{\text{Na}^+}^f / \Delta C_{\text{BSA}} \quad (C_{\text{BSA}} < C_{\text{BSA}}^{\text{ps}}) \quad (2)$$

where $\Delta C_{\text{Na}^+}^f$ is the released concentration of Na^+ ion and ΔC_{BSA} is the increase of BSA concentration.

In the region of $C_{\text{BSA}} < C_{\text{BSA}}^{\text{ps}}$, approximating that almost all BSA molecules added to the NaHA solution bind to NaHA molecules and free BSA molecules can be neglected from the results of Fig. 7, the values of n can be obtained from the slope of C_{Na^+} shown in Fig. 3. The slope was constant in the region of $C_{\text{BSA}} < C_{\text{BSA}}^{\text{ps}}$ and the value of n was found to be 15. One BSA molecule binds with 15 carboxylic groups of NaHA. Since the molecular weight of a repeating unit of NaHA is $401 \text{g} \cdot \text{mol}^{-1}$, there are 2119 carboxylic groups in one NaHA molecule. Then, assuming all carboxylic groups of NaHA bind to BSA, 141 BSA molecules should bind to 1 NaHA molecule for the saturated complex, i.e., $(C_{\text{BSA}}/C_{\text{NaHA}})_{\text{cal}}^{\text{sat}} = 141$. The experimental result of

$(C_{\text{BSA}}/C_{\text{NaHA}})^{\text{ps}} (=117)$ was smaller than the calculated value and 17% of the carboxylic groups were found not to contribute to the formation of the complexes. These free carboxylic groups are considered to contribute to the negative mobility of the complexes ($C_{\text{BSA}} \geq C_{\text{BSA}}^{\text{ps}}$) shown in Fig. 8.

In the region of $C_{\text{BSA}} \geq C_{\text{BSA}}^{\text{ps}}$, the value of n obtained was 6 from the slight increase of C_{Na^+} shown in Fig. 3. BSA molecules were found to bind furthermore to the complex. The charge densities of the complexes approach to zero due to the extra binding to BSA. The decrease in the electrostatic repulsion between the complexes brings about the inter-polymer complex, which is followed by the phase separation.

The Model of Complex Formation The NaHA molecule is a rod- or worm-like structure and the BSA molecule is a prolate ellipsoid one. BSA molecules bind to the carboxylic groups of the NaHA molecules by electrostatic attraction and form intra-polymer complexes. With increasing the binding amounts of BSA, the apparent charge amounts decrease due to the shielding effects and the extensions of NaHA contract, i.e., NaHA molecules are entangled by the bindings of BSA, which induces a decrease in the viscosity and the diffusion coefficients. In the region of $C_{\text{BSA}} \geq C_{\text{BSA}}^{\text{ps}}$, the interactions between complexes are enhanced due to the decreases of the electrostatic repulsion, and inter-polymer complexes are formed and a phase separation occurs. The model of the complex formation is shown in Fig. 9.

The complexes of sodium chondroitin sulfate C (ChS) and BSA were studied using a static light scattering and the shape was reported to be a rod-like structure just like ChS alone. With increasing the binding amounts of BSA, the length was 30% longer and 6 times thicker in diameter than the ChS molecule at the saturated binding state.⁹⁾ Acid mucopolysaccharides are a rod or worm like structure in aqueous solutions due to the electrostatic repulsion of the negative charges and the stiffness of sugar chains. The charge density of ChS is two times as much as NaHA, which might induce the rod-like structure of the complexes of ChS and BSA even at the saturated binding state. On the other hand, the sizes of the complexes of HA and BSA decreased with increasing the binding amounts of BSA. The differences of the shape from the complexes of ChS and BSA are considered to result from the smaller charge densities and the much higher molecular masses of NaHA (M_w of NaHA, $850 \times 10^3 \text{g} \cdot \text{mol}^{-1}$, M_w of NaChS, $70.9 \times 10^3 \text{g} \cdot \text{mol}^{-1}$).

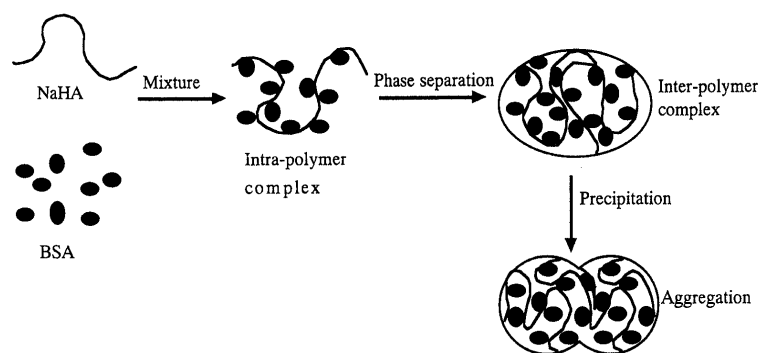


Fig. 9. Model of NaHA-BSA Complex Formation

References

- 1) Chen R. F., *J. Biol. Chem.*, **242**, 173—180 (1967).
- 2) Yonese M., Yano M., *Bull. Chem. Soc. Jpn.*, **64**, 1814—1820 (1991).
- 3) Kokufuta E., Dubin P. L., *Surface*, **32**, 460—479 (1994).
- 4) Yonese M., Xu S. H., Kugimiya S., Sato S., Miyata I., *Prog. Colloid Polym. Sci.*, **106**, 252—256 (1997).
- 5) Makino K., Ikekita M., Kondo T., Tanuma S., Ohshima H., *Colloid Polym. Sci.*, **272**, 478—492 (1994).
- 6) Xia J. L., Dubin P. L., Kim Y., Muhoberac B. B., Klimkowski V. J., *J. Phys. Chem.*, **97**, 4528—4534 (1993).
- 7) Tsuboi A., Izumi T., Hirata M., Xia J. L., Dubin P. L., Kokufuta E., *Langmuir*, **12**, 6295—6303 (1996).
- 8) Yamaguchi K., Hachiya K., Moriyama Y., Takeda K., *J. Colloid Interface Sci.*, **179**, 249—254 (1996).
- 9) Nakagaki M., Sano Y., *Bull. Chem. Soc. Jpn.*, **45**, 1011—1018 (1972).
- 10) Sano Y., *Bull. Natl. Inst. Agrobiol. Resour.*, **2**, 1—12 (1986).
- 11) Lyon M., Nieduszynski I. A., *Biochem. J.*, **213**, 445—450 (1983).
- 12) Izumi T., Hirata M., *J. M. S.-Pureappl. Chem.*, **A31**, 39—51 (1994).
- 13) Anno K., *Comparative Biochemistry of Mucopolysaccharides*, **14**, 167—170 (1977).
- 14) Pouyani T., Harbison G. S., Prestiwich G. D., *J. Am. Chem. Soc.*, **166**, 7515—7522 (1994).
- 15) Isogai Z., Yoneda M., Itan N., Kimata K., *Nagoya Med. J.*, **41**, 27—37 (1997).
- 16) Nonogaki T., Xu S. H., Kugimiya S., Sato S., Miyata I., Yonese M., *Langmuir*, accepted.
- 17) Pecora R., *Dynamic Light Scattering: Application of Photon Correlation Spectroscopy*, Plenum Press, New York, 1976.
- 18) Schmitz K. S., *An Introduction to Dynamic Light Scattering by Macromolecules*, Academic Press, New York, 1990.
- 19) Kratky O., Porod G., *Recl. Trav. Chim. Pays-Bas.*, **68**, 1106 (1949).
- 20) Nakajima A., Shinoda K., *J. Colloid Interface Sci.*, **55**, 126—132 (1976).
- 21) Hagiwara T., Kumagai H., Nakamura K., *Biosci. Biotech. Biochem.*, **60**, 1757—1763 (1996).